

## Comparison of TRMM Precipitation Radar and Kwajalein Ground Validation 3-D Radar Reflectivity Fields

Courtney Schumacher and Robert A. Houze, Jr.  
*Department of Atmospheric Sciences*  
*University of Washington*

The TRMM Precipitation Radar (PR) and Kwajalein ground radar reflectivity fields are compared during concurrent satellite overpasses and radar-observed rain events for August and September 1998. Two cases exhibit significant convective and stratiform rain structures. Qualitative evaluation of horizontal and vertical cross-sections shows that the satellite radar and ground-based radar correspond generally well with similar structures of brightbands and convective cells. Horizontal cross-sections agree in the locations of convective cells and stratiform regions. Discrepancies occur in the thickness of the bright band and the vertical gradients of reflectivity in convective cells. Two possible explanations for these discrepancies are: 1) that the PR and ground radar have significantly different scan strategies and scattering volumes, which make direct comparisons difficult; and 2) PR data were not yet corrected for attenuation. Statistical methods (CFADs) show good agreement between the PR and ground radar in the modes of frequency distributions. CFAD comparisons further highlight the extent of PR attenuation in the convective case and the portion of the ice region that is not detectable by the PR.

### 1. Kwajalein radar site

The Kwajalein radar is S-band and Doppler. It is situated on Kwajalein Island (8.72 N, 167.73 E), which is at the southern tip of the Kwajalein atoll in the Republic of the Marshall Islands (Fig. 1). Data is regularly received from eleven tipping bucket rain gauges located within a 200 km radius of the radar. The Kwajalein radar is ideal for TRMM ground validation because of its oceanic location and its scan strategies that maximize vertical resolution. A typical Kwajalein scan strategy has 22 elevation angles versus the standard NEXRAD scan strategies of nine to 14 (Fig. 2).

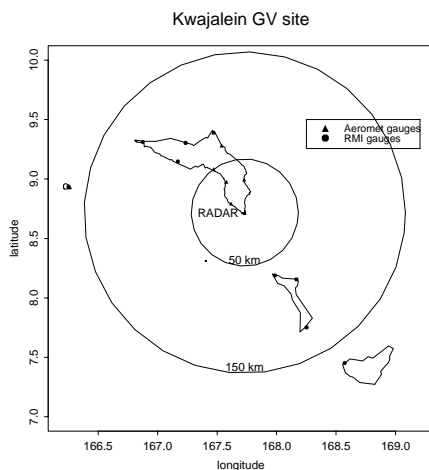


Fig. 1. Map of Kwajalein area.

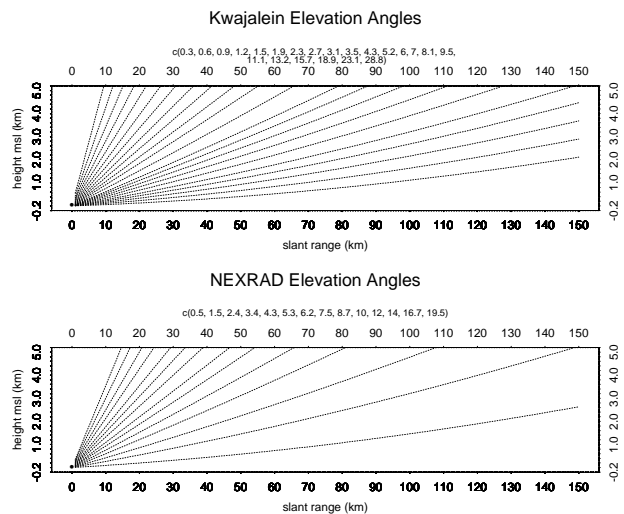


Fig. 2. Scan strategies for Kwajalein and NEXRAD radars. Center of beam is plotted.

## 2. August-September 1998 overpasses

PR data (product 1C21 obtained from TSDIS) and Kwajalein ground radar data were compared for August and September 1998. These months are climatologically rainy, averaging 250-300 mm of rain per month at Kwajalein Island. The PR's 215 km swath overlapped the 150 km radius area surrounding the ground radar roughly 20 times each month. In September, 13 of the 19 overpasses had greater than one-third areal overlap (Fig. 3). Of those 13 cases, only four had average rain rates (calculated from the ground radar) greater than 1 mm/h within the region of overlap. In August, eight of the 14 cases with greater than one-third areal overlap had average rain rates greater than 1 mm/h. Two events were chosen that had both large areal overlap and significant rain amounts, 20 August—ground radar 0520 UTC, PR 0521 UTC (orbit 4184) and 18 September—ground radar 1357 UTC, PR 1400 UTC (orbit 4647). The August event was strongly stratiform while the September event was significantly convective.

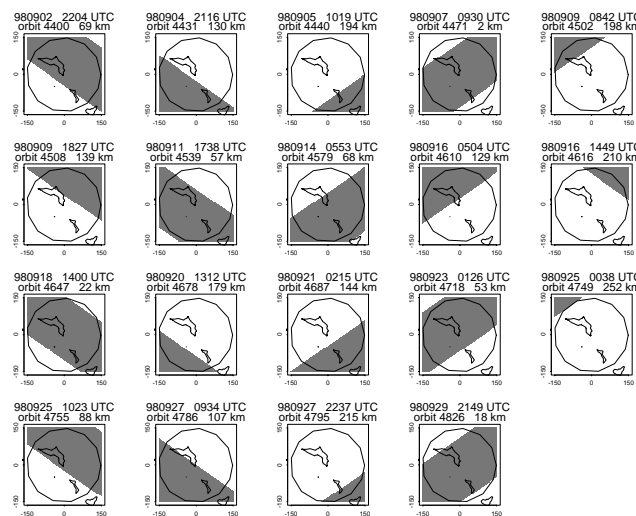


Fig. 3. September 1998 Kwajalein PR overpasses. Circle radius is 150 km, centered on the Kwajalein radar.

## 3. Two cases

Qualitatively, the horizontal and vertical cross-sections for each case compare well between the PR and the Kwajalein ground radar. The ground radar 5 km altitude horizontal cross-section and PR bin 62 cross-section for the August case (Figs. 4 a and b) show matching widespread stratiform echo areas, both in location and relative intensity. Smaller features such as the 15 km x 5 km cell in the NW part of the Kwajalein atoll also match. Vertical cross-sections at PR ray 16 (Figs. 4 c and d) exhibit similar bright band heights and vertical cell structure although the PR bright bands tend to be sharper in the vertical. This is due to the higher vertical resolution of the PR (250 m at nadir) than the ground radar (1000 m at 60 km from the radar along the lowest tilt).

Strong similarities are also seen between the PR and the Kwajalein radar in the September case. The horizontally smaller yet intense convective cells in the ground radar 2.5 km altitude horizontal cross-section and PR bin 62 cross-section (Figs. 5 a and b) agree well in locations and relative intensities. The vertical cross-sections at PR ray 22 (Figs. 5 c and d) show that the convective cells have similar 15 dBZ contour heights. Effects of attenuation are apparent where maximum PR reflectivities are found aloft in the convective cells.

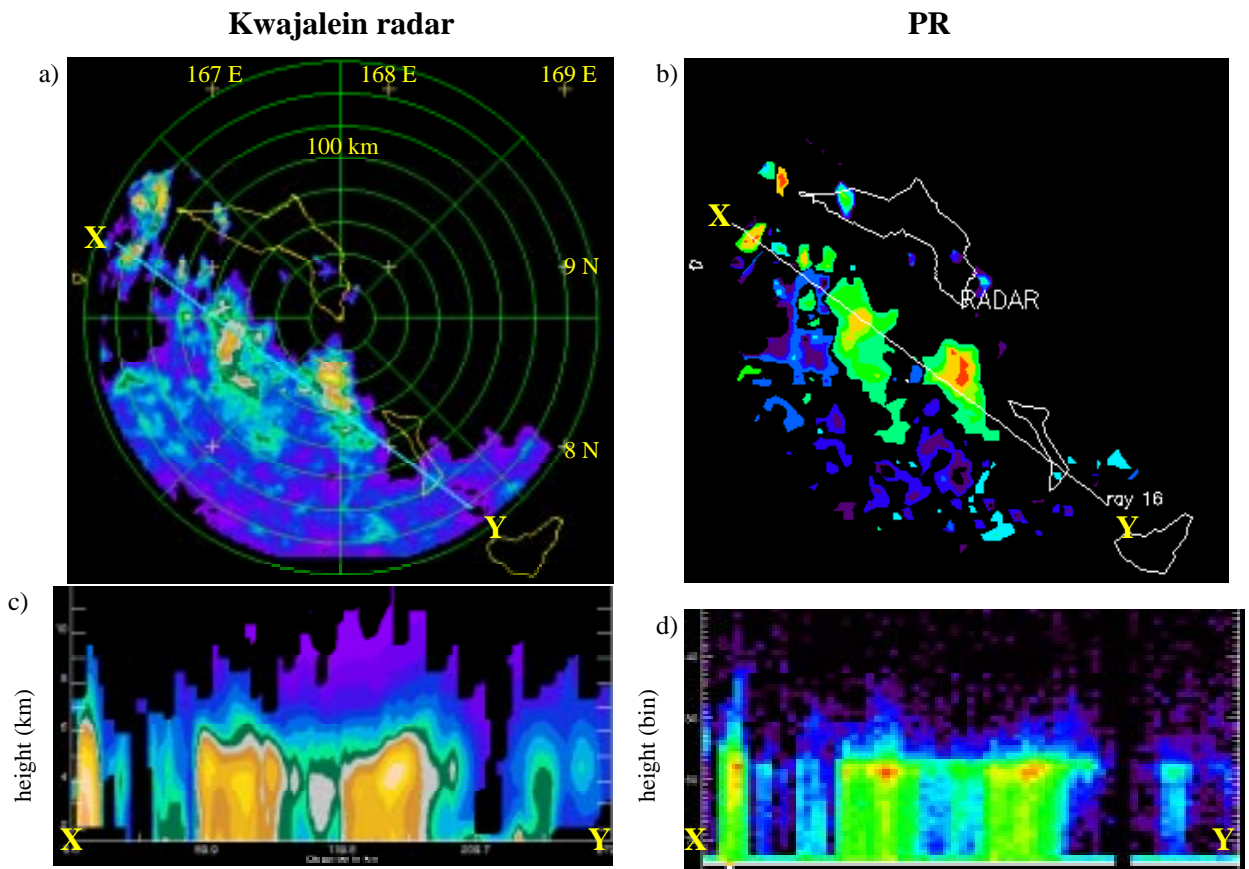


Fig. 4. Stratiform case observed on 20 August 1998 by the Kwajalein ground radar at 0520 UTC and TRMM PR at 0521 UTC (orbit 4184). a) 5 km ground radar cross-section. Reflectivity contour values range from 12-40 dBZ. b) PR bin 62 (~5 km) cross-section. RADAR refers to the Kwajalein ground radar. Reflectivity contour values range from 15-40 dBZ. Horizontal scale is similar to a). c) Ground radar vertical cross-section X-Y. Contour range 0-40 dBZ. d) PR vertical cross-section at ray 16. Pixel range is 15-40 dBZ. Scaling is similar to c) (i.e. bin 50~6 km).

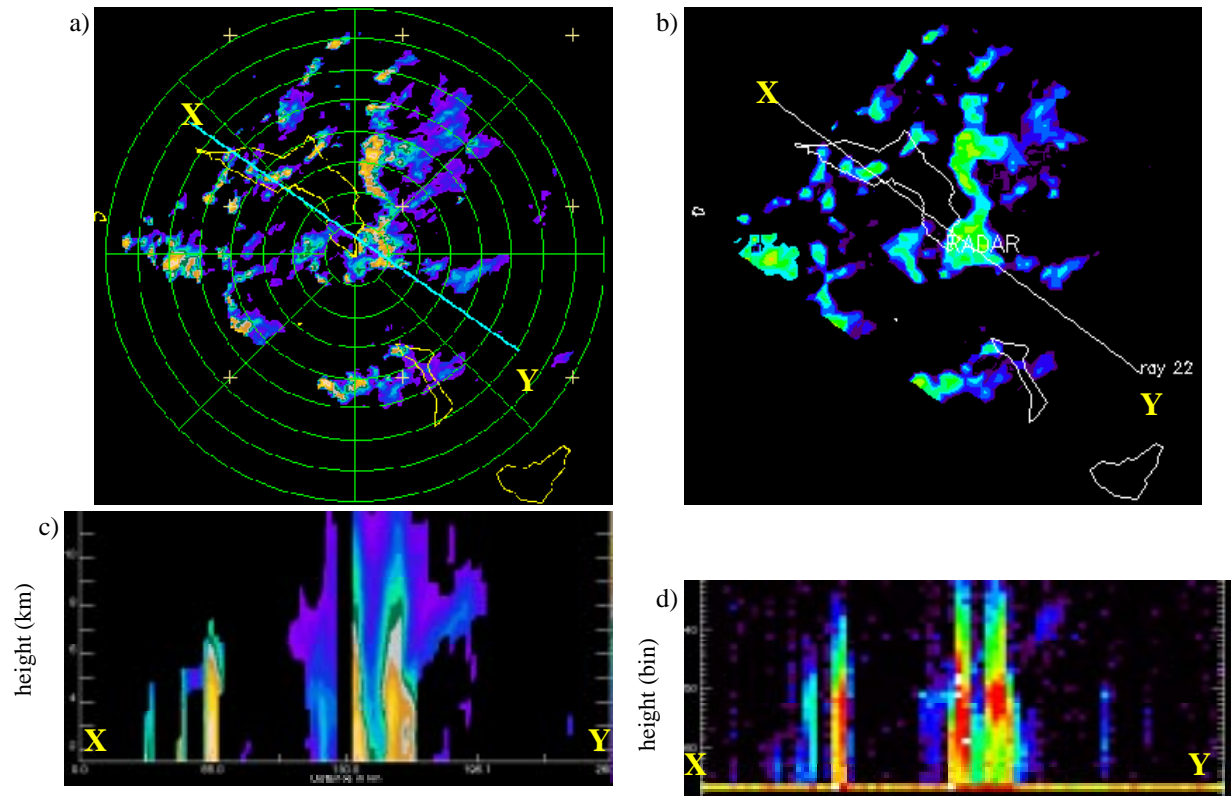


Fig. 5. Convective case observed on 18 September 1998 by the ground radar 1357 UTC and the TRMM PR at 1400 UTC (orbit 4647). Same as Fig. 4 except a) is the 2.5 km cross-section, b) bin 62~2.5 km, d) is PR ray 22 vertical cross-section and bin 50 is ~5 km in altitude.

#### 4. Contoured Frequency by Altitude Diagrams (CFADs)

Quantitative comparison of the PR and Kwajalein radar is difficult because of their significantly different wavelengths, sensitivities, scan strategies and scattering volumes. The PR operates at 13.8 GHz, has a minimum detectable reflectivity of  $\sim 17$  dBZ, is downward looking with 250 m gate spacing, and has a roughly 4 km x 4 km surface footprint. The Kwajalein radar operates at 10 cm, is sensitive to particles  $< 0$  dBZ, is horizontally looking with gate spacing of 250 m, and has beamwidth of  $\sim 1$  degree that spreads to a kilometer at a distance of 60 km from the radar. Using interpolation based on Mohr and Vaughn (1979), the PR and ground radar volumes were mapped to grids of horizontal resolution 4 km and 2 km respectively and 500 m in the vertical. Only data within a 100 km radius of the Kwajalein radar was used.

The PR and ground radar CFADs for the two example cases show good agreement within the range of the PR's sensitivity ( $> 17$  dBZ). The stratiform CFADs from August (Figs. 6 a and b) both show a tendency for maximum reflectivity just below the  $0^{\circ}\text{C}$  level ( $\sim 5$  km) with a narrow distribution marked by packed contours just above. A mode at  $\sim 20$  dBZ decreasing downward is seen beneath the freezing level on both radars, and there is a hint of the ground radar's ice region mode in the PR CFAD. The convective PR CFAD from September (Fig. 6 c) exhibits a broad distribution (loose contours), and again the ground radar's ice mode is suggested (Fig. 6 d). Frequency contours in the PR convective case have decreasing reflectivity approaching the surface as opposed to the tendency for a low-level maximum seen in the ground radar CFAD. This latter comparison indicates attenuation of the PR.

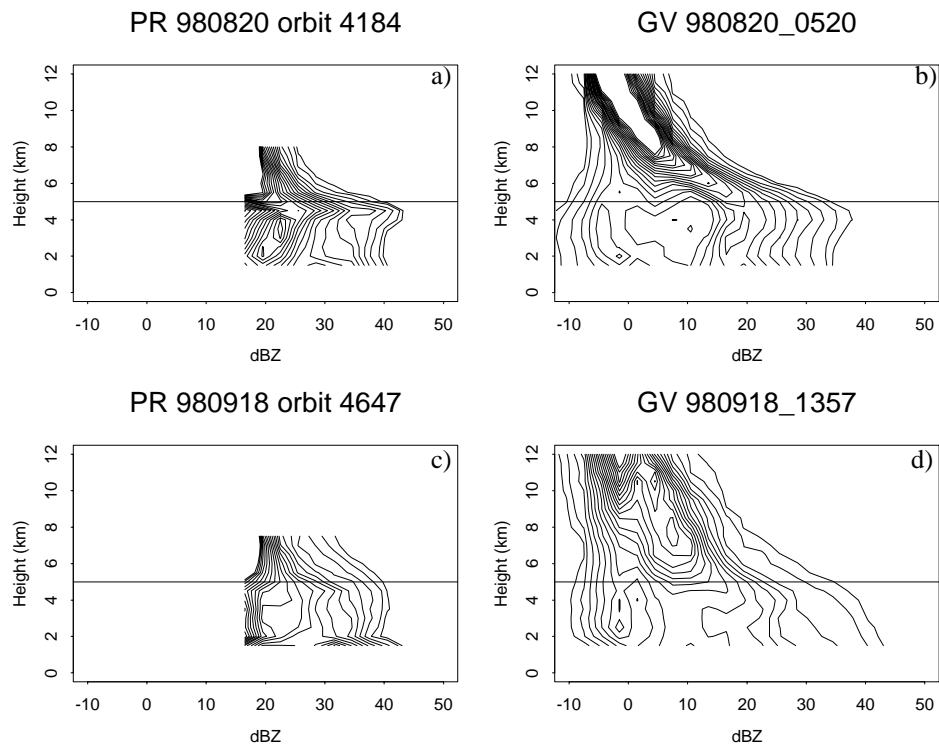


Fig. 6. CFADS representing the August stratiform case and September convective case.  
a) PR 20 Aug 0521 UTC. b) Ground radar 20 Aug 0520 UTC. c) PR 18 Sept 1400 UTC.  
d) Ground radar 18 Sept 1357 UTC.

## 5. Microphysics

Much microphysical information can be gleaned from CFADs (e.g. Yuter and Houze 1995). Contours in the stratiform CFADs (Figs. 6 a and b) show a narrow distribution of reflectivity at any given height above the freezing level. The mode of this narrow distribution increasing downward is consistent with ice particles drifting downward, growing at higher levels by vapor deposition and then by aggregation closer to the 0°C level, thus producing higher reflectivities. The convective CFADs (Figs. 6 c and d) have a broad distribution (loose contours) aloft. Higher reflectivities in this broad distribution aloft indicate a predominance of graupel, consistent with convective drafts favoring growth of particles by riming. The convective case has a mode with a more vertical slope in the ice region than the stratiform case which suggests aggregation wasn't an important process. The mode decreasing downward beneath the freezing level in the stratiform case possibly indicates evaporation.

## 6. Conclusions

Qualitative evaluation of the PR and Kwajalein radar for each storm generally showed good agreement between the two radars in both the vertical and horizontal cross-sections. Some differences were evident in the vertical gradients of reflectivity between the two radars. However, the use of attenuation corrected data and appropriate interpolation techniques may compensate for these differences.

Statistical comparison in the form of CFADs showed that within its range of sensitivity, the PR can indicate the general microphysical nature of a storm. However, ground validation radars are important in their ability to supplement the satellite data. The ground radar at Kwajalein covers a much deeper and broader region of ice-filled atmosphere than can the PR. The Kwajalein radar also employs a large number of elevation angles to cover the ice region in detail and it scans continuously in time, so the development of the ice region is documented. The Kwajalein ground radar thus provides a detailed and complete microphysical context, which will allow for better physical interpretation of the PR data.

*Acknowledgments.* We received essential scientific and computational help from Stacy Brodzik and Sandra Yuter. This research was supported by NASA #NAG5-4795.

## References

- Mohr, C. G. and R. L. Vaughan, 1979: An Economical Procedure for Cartesian Interpolation and Display of Reflectivity Factor Data in Three-Dimensional Space. *J. Appl. Meteor.*, **18**, 661-670.
- Nakamura, K., K. Okamoto, T. Ihara, J. Awaka, T. Kozu, T. Manabe, 1990: Conceptual Design of Rain Radar for the Tropical Rainfall Measuring Mission. *Internatl. J. Satellite Communications*, **8**, 257-268.
- Yuter, S. E. and R. A. Houze Jr., 1995: Three-dimensional kinematic and microphysical evolution of Florida cumulonimbus. Part II: Frequency Distributions of Vertical Velocity, Reflectivity, and Differential Reflectivity. *Mon. Wea. Rev.*, **123**, 1941-1963.